ENVIRONMENTAL RESEARCH
LETTERS

LETTER • OPEN ACCESS

Changes in building climate zones over China based on high-resolution regional climate projections

Environmental Research Letters

CrossMark

OPEN ACCESS

RECEIVED
11 June 2020

REVISED
14 September 2020

ACCEPTED FOR PUBLICATION
2 October 2020

PUBLISHED
18 November 2020

LETTER

Changes in building climate zones over China based on high-resolution regional climate projections

Ying Shi[1] **and Guiling Wang**[2]

[1] National Climate Center, China Meteorological Administration, Beijing, People's Republic of China
[2] Department of Civil and Environmental Engineering, and Center for Environmental Sciences and Engineering, University of Connecticut, Storrs, United States of America

E-mail: shiying@cma.gov.cn

Keywords: climate change, building climate zone, climate classification, regional climate model, China

Abstract

Based on the up-to-date observations and five sets of high-resolution climate projections under RCP4.5 over East Asia using a regional climate model, this study defines building climate zones over China and assesses their past and future changes according to an established climate classification scheme. The five-model ensemble captures the observed general distribution of climate zones, with a distinct latitudinal pattern over the densely populated eastern China, a subarctic zone in the western mountains including the Tibetan Plateau and a cool dry zone in the Tarim and Turpan basins; large disparities are found in northwestern China due to warm and dry biases. Observational data identifies a recent northward shift of most climate zones in eastern China and a shrinking of the subarctic climate zones over the Tibetan Plateau, which caused a building climate zone change for 18% of the country's land area. As the warming continues in the future, the five-model ensemble projects additional climate zone changes influencing 43% and 55% of the country by mid- and late-century, respectively. In addition, the total area of the subarctic zone is projected to decrease from 16.6% of the country in present-day climate to 9.2% and 7.4% in the mid- and late-century, respectively, and that of the hot or very-hot climate zone is projected to expand from 4.2% to 9.1% and 11.3%, respectively. These changes should be taken into consideration in long-term development planning related to urbanization, energy efficiency, and environmental sustainability.

1. Introduction

The Fifth Assessment Report (AR5) of the Intergovernmental Panel on Climate Change (IPCC) found that 'warming of the climate system is unequivocal'. Global average of surface temperature shows a warming of 0.85 [0.65–1.06]°C over the period of 1880 to 2012, with faster warming in recent decades. Further warming which is estimated to be in the range of 0.3 °C–4.8 °C averaged in the global by the end of the century (2081–2100) relative to the present day (1986–2005) is projected with continued emission of greenhouse gases (GHGs) (IPCC 2013). One of the potentially more significant effects of climate change is the alteration of the distribution, speciation and life cycle of vegetated ecosystems (IPCC 2013). As a simple method to combine the climate variables and vegetation, climate classification such as the Köppen climate classification (Köppen 1936) and its modified versions Köppen–Geiger (K-G, Kottek *et al* 2006), Köppen–Trewartha (K-T, Trewartha and Horn 1980), and the cluster analysis (Zhang and Yan 2014, Netzel and Stepinski 2016) has been frequently used in a broad range of topics concerning climate and climate change impact as they related to biogeography, hydrology, horticulture, agriculture, and engineering design (e.g. Kottek *et al* 2006, de Castro *et al* 2007, Gao and Giorgi 2008, Ruble and Kottek 2010, Baker *et al* 2010, Jacob *et al* 2012, Shi *et al* 2012, Chen and Chen 2013, Feng *et al* 2014, Zhang *et al* 2017, Fermandez *et al* 2017, He *et al* 2019). The choice of classification often depends on the application purpose. For example, in the U.S., the USDA Hardiness zone is used for horticulture and agriculture (USDA Plant Hardiness Zone Map 2012), and the building zone classification for energy efficiency is based on temperature, precipitation, and heating and cooling degree days (HDD and CDD) (ANSI/ASHRAE Standard 169 2013).

Similar to the Köppen climate classification, climate zones in China are defined according to a set of rules (e.g. NMA 1979, 1994, 2002, EBCAS 1985). The climate classification for building design started in the 1980s, and the latest standard of climate regionalization for architecture was released in 1993 (MCC 1993). This building design standard is defined according to the mean temperature in January and July, the cumulative days of daily temperature higher or lower than a certain threshold, the annual total precipitation, and the maximum wind. Following the 1993 standard, the spatial distributions of the building climate zones have been investigated based on observed climate (e.g. Fu *et al* 2008, Bai and Yang 2018). With the modernization of China's infrastructure, building energy efficiency has become increasingly important, and new approaches towards the development of building climate zones for China have emerged. For example, Bai *et al* (2020) investigated the applicability of the ANSI/ASHRAE Standard to climate in China and proposed additional zones to identify high elevation as the cause for cool, cold, and very cold zones in regions such as the Tibetan Plateau. In this study we examine how future climate change may influence the building climate zones according to the ANSI/ASHRAE Standard.

In a warming world, climate zones are expected to migrate with the changes of temperature and precipitation. To investigate the response of the climate system to increases in GHG concentrations and to project future climate, the primary tools are coupled global atmosphere-ocean general circulation models (GCMs). Based on the simulations from the global models, changes of climate zones have been analyzed by many researchers. For example, using the K-G classification, Rubel and Kottek (2010) generated a series of digital world maps for the extended period 1901–2100 and showed the largest shifts between the main classes of equatorial climate (A), arid climate (B), warm temperate climate (C), snow climate (D) and polar climate (E) on global land areas are estimated to be 2.6%–3.4% (E to D), 2.2%–4.7% (D to C), 1.3–2.0 (C to B) and 2.1%–3.2% (C to A). Feng *et al* (2014) indicated that the K-T climate types would shift toward warmer and drier climate types from the current climate distribution based on CMIP5 models. Belda *et al* (2016) found a substantial decline in ice cap, tundra, and boreal climate in the warming world, accompanied by an expansion of temperate climates, dry climates, and savanna, nearly unanimous within the CMIP5 ensemble.

Generally, a model with higher resolution performs better compared to its lower-resolution counterpart (Gao *et al* 2006, Shi *et al* 2018). With the rapid increase of computational capacity, high-resolution models are becoming increasingly common in Phases 5 and 6 of the Coupled Model Intercomparison Project (CMIP5, Taylor *et al* 2012; CMIP6, Eyring *et al* 2016). But the resolution is still too coarse to capture the effects of local and regional forcing, especially in regions with complex topography such as China, leading to model performance challenges (e.g. Jiang *et al* 2005, Xu *et al* 2010, Yu *et al* 2011). From the application side, coarse resolution global models cannot resolve the spatial heterogeneity needed for developing local and regional climate adaptation strategies. Nested high-resolution regional climate modeling (RCM) has been used to improve simulation fidelity and to better represent the spatial heterogeneity over China (e.g. Gao *et al* 2001, 2006, 2013, Qian and Leung 2007, Zou and Zhou 2013). However, few high-resolution studies on climate classification have been conducted in general and for building energy efficiency purpose over China in particular.

In this paper, climate classifications used for building code and energy efficiency will be analyzed based on five sets of high-resolution climate change simulations under RCP4.5 scenario over East Asia using the regional climate model version 4.4 (RegCM4.4) driven by five different global models of CSIRO-Mk3-6-0, EC-EARTH, HadGEM2-ES, MPI-ESM-MR and NorESM1-M (Han *et al* 2017, Gao *et al* 2018, Shi *et al* 2018). Multi-model ensemble mean has been shown to outperform individual models (Pierce *et al* 2009, Feng *et al* 2014) and is used here to reduce model-related uncertainties. Section 2 describes the model, data, experimental design, and the definition of building climate zones. The observed changes, the model validation and future changes of climate types are shown in section 3. The main conclusions and discussions are presented in section 4.

2. Methods

2.1. Model, data and experimental design

The Abdus Salam International Centre for Theoretical Physics (ICTP) Regional Climate Model, RegCM4.4 (Giorgi *et al* 2012) is employed in this study. The grid spacing is 25 km and the vertical sigma layers are 18 with a model top at 10 hPa. The simulation period is 1981–2100 plus 3 years of spin-up time in the beginning, with CO_2 concentrations varying as observed before 2005 and following the RCP4.5 scenario (Moss *et al* 2010) afterwards. The model domain is the same as the Phase II East Asia domain of the international Coordinated Regional climate Downscaling Experiment (Giorgi *et al* 2009), which includes China and the surrounding areas. Other model physics include the land surface scheme CLM3.5 (Oleson *et al* 2008), the convection scheme of Emanuel (Emanuel 1991), the non-local formulation of Holtslag *et al* (1990) for planetary boundary layer, resolvable scale precipitation scheme of Pal *et al* (2000), and the NCAR community climate model

Table 1. The five global climate models used to drive regional climate downscaling.

Model/Country	Resolution (longitude × latitude)	Reference
CSIRO-Mk3-6-0/Australia	192 × 96	Rotstayn *et al* 2010
EC-EARTH/Europe	320 × 160	Hazeleger *et al* 2010
HadGEM2-ES/UK	192 × 145	Collins *et al* 2011
MPI-ESM-MR/Germany	192 × 96	Stevens *et al* 2012; Jungclaus *et al* 2013
NorESM1-M/Norway	144 × 96	Bentsen *et al* 2013; Iversen *et al* 2013

CCM3 for the atmospheric radiative transfer scheme (Kiehl *et al* 1998).

The initial and boundary conditions at six hourly intervals are needed to drive the RegCM4.4 model which is usually derived from GCMs. The ratio of the RCM to GCM resolutions should be less than 10, and preferably in the range of 3–5. Considering model resolution, performance over the domain of interest, model climate sensitivity, and data availability for desired RCPs, we selected five CMIP5 global models to include in this study, CSIRO-MK3-6-0, EC-EARTH, HadGEM2-ES, MPI-ESM-MR and NorESM1-M (table 1). Note that NorESM1-M, MPI-ESM-MR, HADGEM2-ES are considered the highest priority of GCMs for inclusion in the CORDEX CORE simulations (https://cordex.org/experiment-guidelines/cordex-core/cordex-core-simulation/). In addition, previous studies have shown that the five global climate models have a good performance over China (Zhou *et al* 2014, Jiang *et al* 2016).

Of the 120 years' simulation, the period of 1986–2005 is considered as the historical reference, and changes relative to the historical reference are defined for both the middle-century (2046–2065) and late-century (2080–2099), respectively. The observational temperature and precipitation dataset (CN05.1) developed by Wu and Gao (2013) at 0.25° × 0.25° (latitude by longitude) resolution has been updated to cover the period 1961–2018, and is employed in this study to validate model performance and to quantify past changes of climate zones. It is worth to be mentioned that the performance of the RCM has been evaluated in previous studies (Han *et al* 2017, Gao *et al* 2018, Shi *et al* 2018, Wu and Gao 2020). Therefore, in this paper, we focus on the simulations and future changes of climate zones based on results from the RCM without presenting the model validation for climate simulation.

2.2. Bias correction

Just like global models, climate from RCMs need to be corrected for biases to obtain more realistic estimates of relevant variables to support adaptation assessment (Rahimi *et al* 2019). Therefore, prior to their application in building climate zone assessment, the RCM outputs went through a two-step bias correction procedure (Han *et al* 2019) making use of the climatological annual cycle derived from the daily data of CN05.1. Specifically, following a similar approach of Kim *et al* (2016), the model-based anomalies were first interpolated to the CN05.1 grid and added to the CN05.1 annual cycle to derive an intermediate dataset that has the same climatology as CN05.1 and same anomalies as the model. Quantile delta mapping (QDM, Cannon *et al* 2015) was then employed to correct the systematic biases in the RCM output, especially in the cumulative distribution function of the simulated variable, using the CN05.1 data as the observational reference. Briefly, the method is based on calculating the relationship between model simulations and observations during the historical period and applying the derived correction factors to future climate projections.

As reported by previous studies, the conventional quantile mapping (QM) method effectively removes the model biases in mean temperature and precipitation, interannual variability, and extreme events (Tong *et al* 2017, Han *et al* 2018) and the bias-corrected results has been used in the projection of the thermal comfort conditions over China (Gao *et al* 2018). Furthermore, Tong *et al* (2020) compared the results after bias correction using the methods of QDM and QM with the original output from the RCM and the results show that both the QM and QDM methods are effective in removing the systematic model biases. It should be noted that the QDM method conserves the future change signal in quantiles simulated by the RCM while the QM does not.

2.3. Climate zones classification scheme

As well known, climate has a great impact on the energy use of residential buildings. In different climate zones, the requirements, such as wall insulation are different (Athalye *et al* 2016). The building climate zone classification approach from the U.S. Department of Energy Pacific Northwest National Laboratory (PNNL) (https://eere.energy.gov/buildings/publications/pdfs/building_america/climate_region_guide.pdf) is based on temperature, precipitation, as well as HDD and CDD due to their relevance to buildings' energy consumption and efficiency. The zones range from 1 in the hottest to 8 in the coldest regions and most are further divided into subzones (table 2). The HDD18 °C and CDD10 °C in the criteria for climate zones are defined as follows:

HDD18 °C: the sum of the absolute difference between 18 °C and the daily mean temperature for 1 d when the mean temperature is less than 18 °C.

Table 2. Definition of climate zones, following the ANSI/ASHRAE Standard 169 (2013).

Zone number	Climate zone	Criteria
1	Very Hot-Humid[(a)] (1 A)/Dry[(b)] (1B)/Marine[(c)] (1 C)	5000 < CDD10 °C
2	Hot-Humid (2 A)/Dry(2B)/Marine(2 C)	3500 < CDD10 °C ≤ 5000
3A and 3B	Warm-Humid (3 A)/Dry(3B)	2500 < CDD10 °C < 3500
3C	Warm-Marine(3 C)	CDD10 °C ≤ 2500 and HDD18 °C ≤ 2000
4A and 4B	Mixed-Humid (4 A)/Dry(4B)	CDD10 °C ≤ 2500 and HDD18 °C ≤ 3000
4C	Mixed-Marine(4 C)	2000 < HDD18°C < 3000
5	Cool-Humid (5 A)/Dry(5B)/Marine(5 C)	3000 < HDD18 °C ≤ 4000
6	Cold-Humid (6 A)/Dry(6B)/Marine(6 C)	4000 < HDD18 °C ≤ 5000
7	Very cold	5000 < HDD18 °C ≤ 7000
8	Subarctic	7000 < HDD18 °C

[a]Moist (A): Locations that are not marine (C) and not dry (B).[b]Marine (C): Locations meeting all four of the following criteria: (1) Mean temperature of coldest month between −3 °C and 18 °C; (2) Warmest month mean temperature <22 °C; (3) At least 4 months with mean temperatures over 10 °C; (4) Dry season in summer. The month with the heaviest precipitation in the cold season has at least three times as much precipitation as the month with the least precipitation in the rest of the year. The cold season is October through March in the Northern Hemisphere and April through September in the Southern Hemisphere.[c]Dry (B): Locations meeting the following criteria: $P < 20.0 \times (T + 7)$ where P is annual precipitation in cm and T is annual mean temperature in °C.

CDD10 °C: the sum of the absolute difference between the mean temperature for 1 d and 10 °C when the mean temperature is more than 10 °C.

Within the U.S., these climate zones were set along county boundaries, making it easier for builders to determine the climate zone building code that a specific neighborhood is subject to; in this study, similar to other climate classifications used in China, boundaries of municipal administration units are not considered. To define climate zones based on the five-model ensemble, the HDD and CDD are first estimated separately for each model and their averages among the five models are then used to classify the climate zones.

3. Results

3.1. Climate zones and past changes

As the observational data is available during 1961–2018, we divide the record into two periods of approximately 30 years, 1961–1990 and 1991–2018. The spatial distribution of the climate zones over China in the two periods and the difference between them are shown in figure 1. Note that changes of all the climate types are analyzed, with a focus on the major 13 groups; climate zones 1B, 1C, 2B, 2C, 5C and 6C each occupies less than 0.1% of the domain and are not shown in the figure.

Distinct latitudinal distribution of climate zones over East China can be found in figure 1(a) and (b), with the hot climate zone (2A) in the south, warm-humid climate zone (3A) in much of the Yangtze River Basin, mixed-humid climate zone (4A) in the Huanghuai River Basins, cool-humid climate zone (5A) along the Taihang Mountain, cold-humid climate zone (6A) extending from the south of the northeast to east of Tibetan Plateau, and the very cold (7) and subarctic climate zones (8) in northeastern China. In western China, subarctic climate zone is dominant in the mountains including the Tibetan Plateau while cool dry climate zone (5B) is found in the Tarim and Turpan basins. Comparison between the two periods indicates that warming during the past several decades has caused a general northward shift of the climate zones (including 1A, 2A, 3A, 4A, 5A, 6A and 7 in eastern China) with an expansion of the spatial coverage for most of them and the greatest decrease in spatial coverage of the zone 8 (subarctic) (figures 1(c) and 2). The climate zone 8 in some parts of the Tibetan Plateau has been replaced by zone 7, and zone 4B in the western basins has increased. The spatial coverage of 4B in the two periods is 0.1% and 1.3%, respectively (figure 2). Taking all changes together, over the past several decades, about 18% of the country has experienced a shift of building climate zone. As the GHG-induced warming continues in the future, more areas of the country will be influenced.

3.2. Model validation and future projections

The climate zones based on the five-model ensemble are compared against the observed data from CN05.1 in figure 3. Different from the 30-year interval used in section 3.1, here the period 1986–2005 is used as the historical reference, following the IPCC AR5 convention (IPCC 2013). The five-model ensemble mean reproduces the spatial distribution of the climate zones over China reasonably well (figures 3(a) and (b)). And it also performs generally better compared to the ensemble mean without bias correction, especially in Northwest China, Southwest China and the Tibetan Plateau (figures not shown). Compared with the observation, the largest differences are found mainly in northwestern China where the model features a greater coverage of 4B while observations feature a greater coverage of 5B, which results from a combination of warm and dry biases of the RCM (Gao *et al* 2018, Shi *et al* 2018). The five-model ensemble mean also well captures the spatial coverage of the climate zones over China, characterized by the maximum percentage (>20%) of very cold

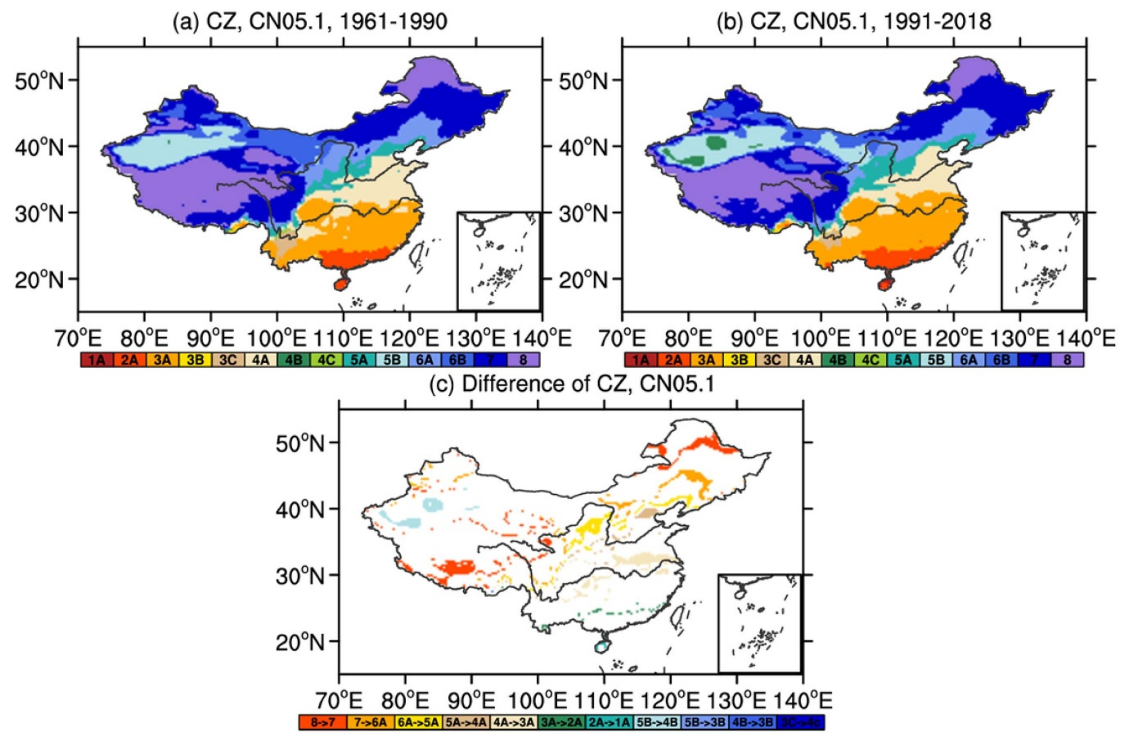

Figure 1. Spatial distribution of the building climate zones over China during 1961–1990 (a) and 1991–2018 (b), and the differences between the two periods (c).

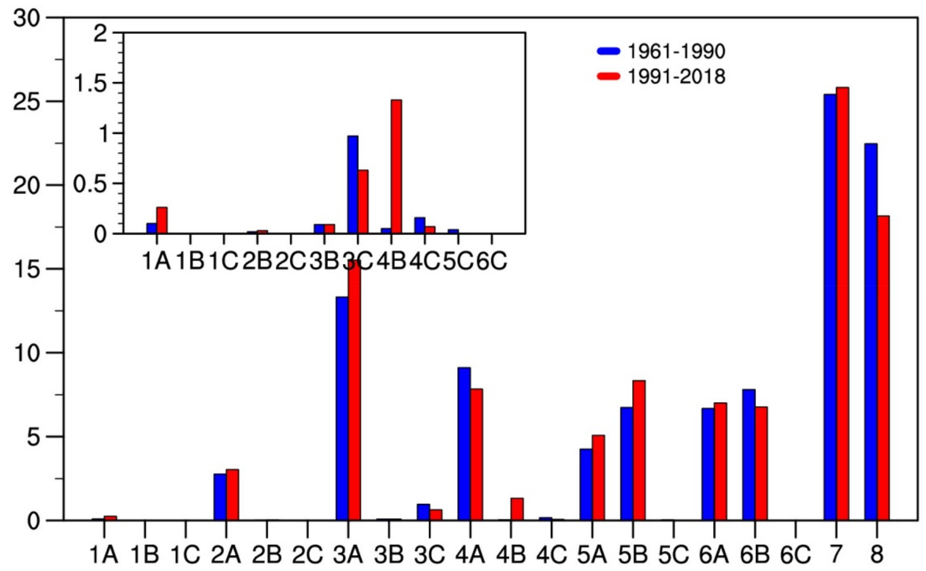

Figure 2. Fractional coverage of the building climate zones (%) in the two historical periods. Building climate zones with a fractional coverage below 2% are shown in the inset.

climate zone, and then the subarctic, the warm, the cold, the cool, the mixed, the hot and the very-hot climate zones (figure 4)

The spatial pattern of climate zones and their projected changes by the mid- and late- century based on the multi-model ensemble mean are shown in figures 3(c)–(f). Relative to the historical reference, significant decrease of the subarctic climate zone and increase of the very-hot and hot climate zones are projected, with greater changes in the late-century than mid-century (figures 3(c) and (d)). Specifically, the fractional coverage of the subarctic zone is projected to decrease from 16.6% to 9.2% and 7.4% by the mid- and late-century, respectively, while that of the very-hot (hot) climate types is projected to increase from 0.3% (3.9%) to 1.0% (8.1%) and 1.5% (9.8%), respectively (figure 4). The overall fractional coverage of the very cold climate zone would decrease from a historical reference of 24.7% to 23.1% and 22.4% in mid- and late-century, respectively, but greater

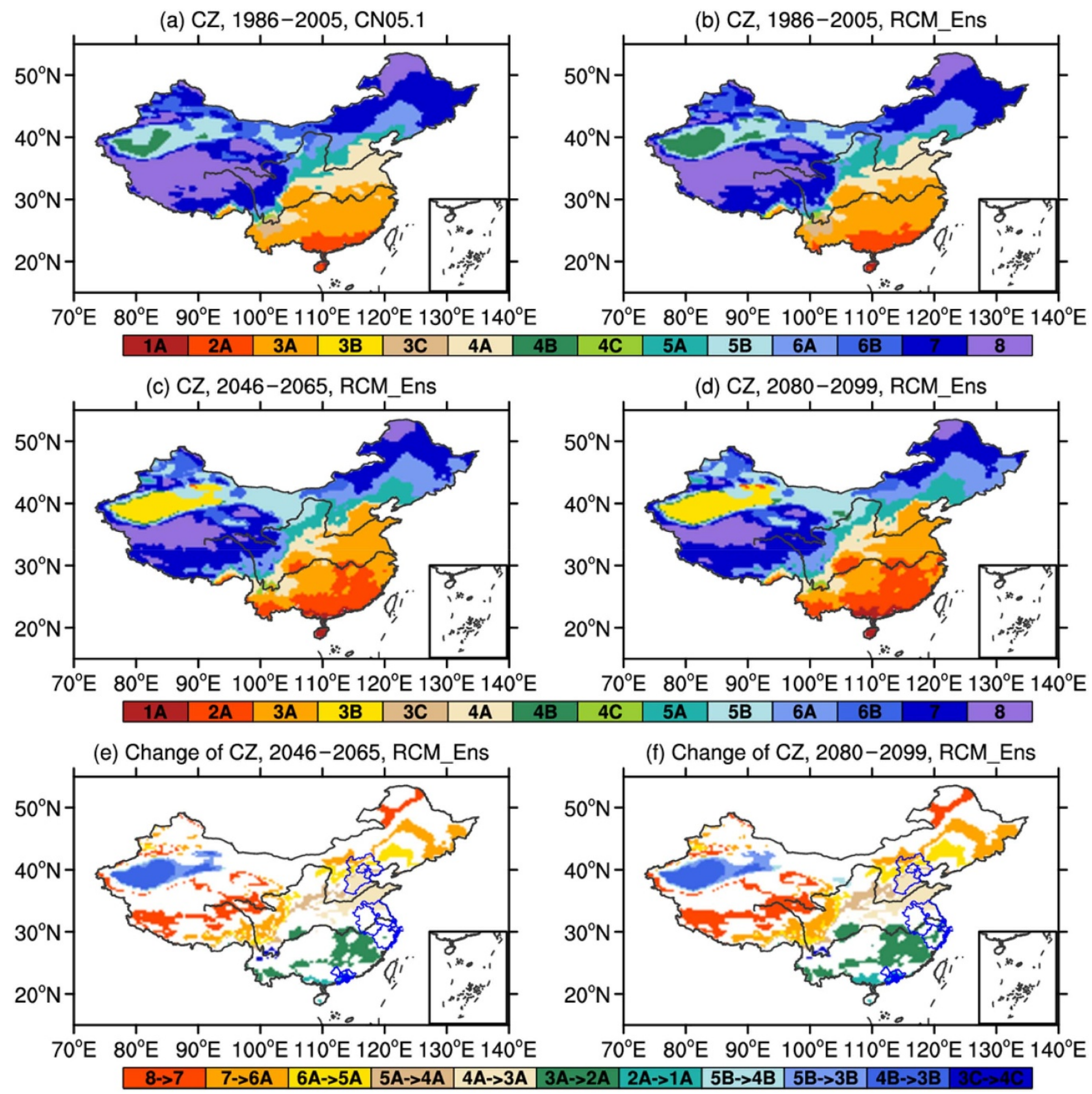

Figure 3. Spatial distribution of the climate zones (a)–(d) and its changes (e)–(f) by the mid- and late-century relative to the historical reference. The magenta solid lines in panels 3e and 3 f outline three major economic regions over East China, Beijing-Tianjin-Hebei, the Yangtze River Delta and the Pearl River Delta from north to south.

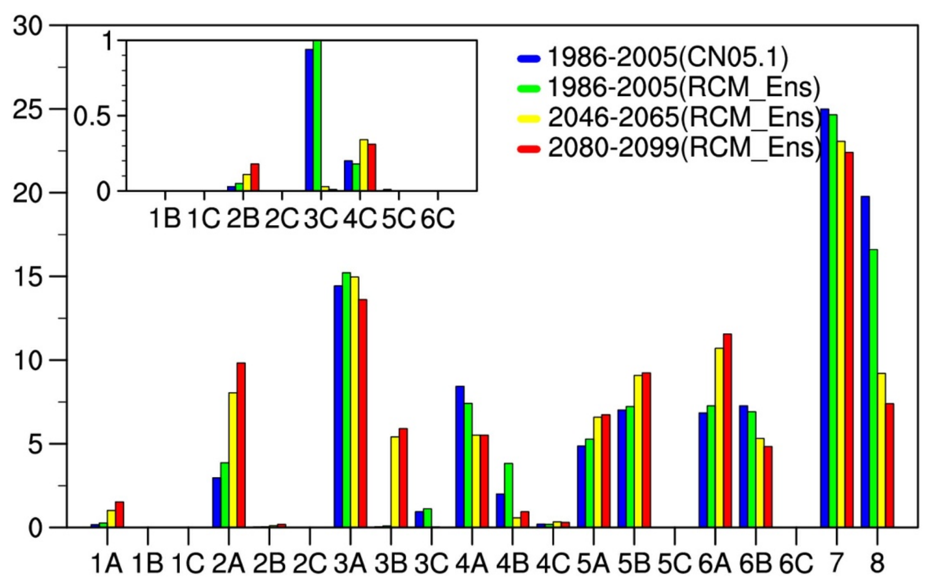

Figure 4. Fractional coverage of the building climate zones (%) in the periods of 1986–2005, 2046–2065 and 2080–2099.

Table 3. Percentage coverage of climate zones in the three periods of 1986–2005 (RF), 2046–2065 (Mid) and 2080–2099 (End) and climate zone changes by the mid- and late-century in the three major economic regions of Beijing-Tianjin-Hebei (JJJ), Yangtze River Delta (YRD) and Pearl River Delta (PRD).

	Percentage coverage of each climate zone									
	JJJ					**YRD**			**PRD**	
	3A	**4A**	**5A**	**6A**	**7A**	**2A**	**3A**	**4A**	**1A**	**2A**
RF	0	44	24	20	12	0	84	16	0	100
Mid	41	13	25	18	3	3	97	0	47	53
End	48	9	25	17	0	21	79	0	62	38
	Percentage coverage of climate zone changes									
	JJJ					**YRD**			**PRD**	
	4A- > 3A	**5A- > 3A**	**5A- > 4A**	**6A- > 5A**	**7A- > 6A**	**3A- > 2A**	**4A- > 3A**		**2A- > 1A**	
Mid	39	1	9	12	9	3	16		47	
End	43	5	8	15	12	21	16		62	

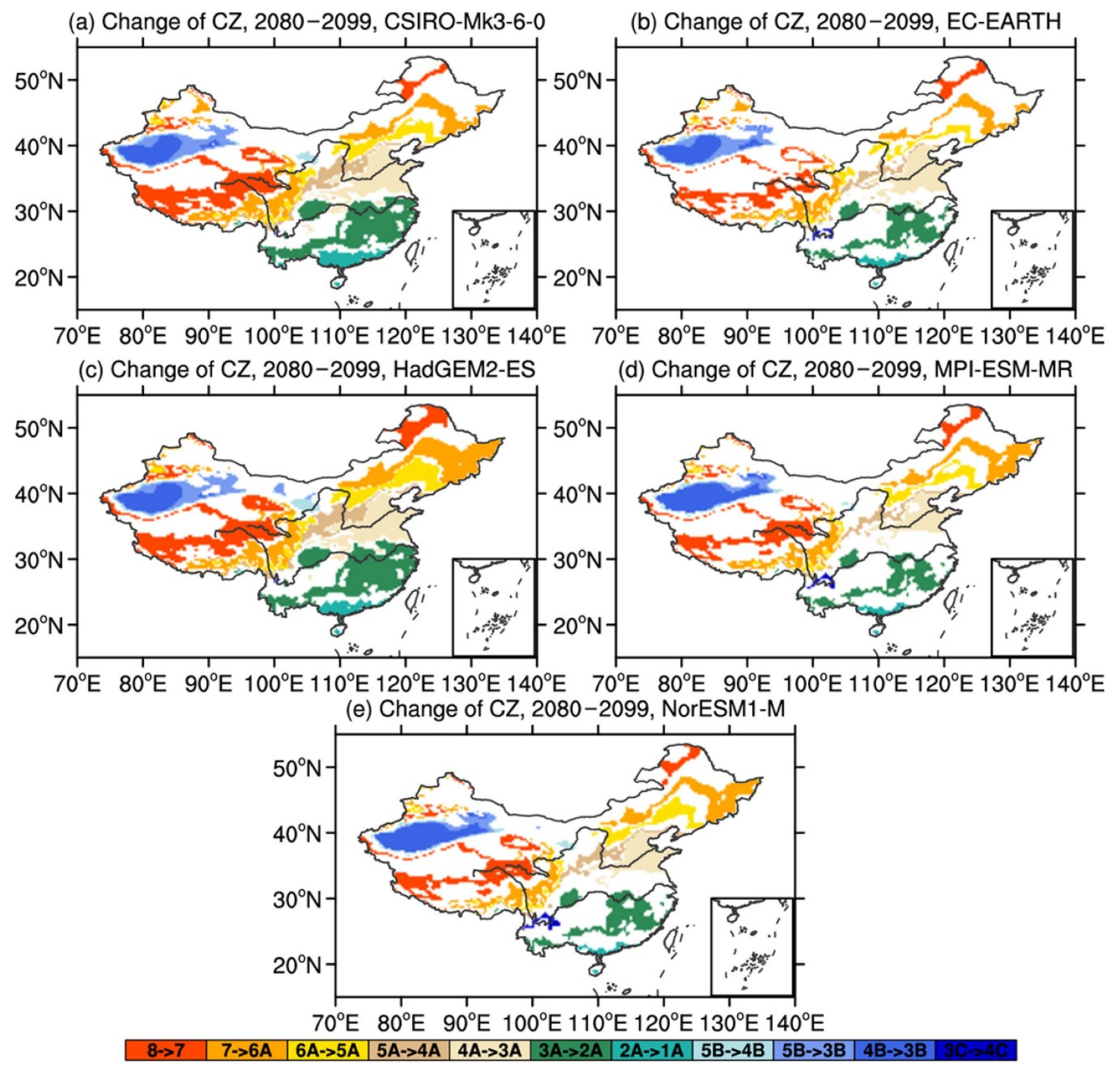

Figure 5. Spatial distribution of the climate zone changes by the late-century relative to the historical reference, simulated by the RegCM model driven by the global models of (a) CSIRO-Mk3-6-0, (b) EC-EARTH, (c) HadGEM2-ES, (d) MPI-ESM-MR, and (e) NorESM1-M.

differences can be found in the spatial distribution, with a decrease in northeast China and an increase in the Tibetan Plateau (figures 3(c) and (d)).

The projected warming would cause a widespread change of the building climate zones associated with a northward shift of the boundaries for climate zones including 1A, 2A, 3A, 4A, 5A and 6A in eastern China, and an extension of 3B in the southern part of Northwest China (figures 3(e) and (f)). These widespread changes towards warmer and more humid building climate zones are projected to influence 43% of the country by the mid-century and 55% by the late-century. The climate zone changes are especially striking in the densely populated regions in eastern China with rapid urbanization and widespread construction (table 3). For example, over the Jing-Jin-Ji region, climate zone 3A is absent in the present day, but is projected to cover 41% and 47% of the region by the mid- and late-century, respectively (table 3). The increase is mainly caused by the change from 4A to 3A due to warming. Other changes from cold to hot climate zones are also found, including from 7A to 6A, 6A to 5A and 5A to 4A. Summing up all changes together, 72% (mid-century) or 83% (late-century) of the region are projected to experience a change of building climate zone. Similarly, 37% of the Yangtze River Delta region is projected to experience a building climate zone change by late-century, when the area of climate zone 2A would increase from zero in the present day to 21% of the region and the climate zone 4A would be completely replaced by 3A (table 3). The whole Pearl River Delta region belongs to zone 2A in the present day, and 62% of it would shift to 1A by the late-century. According to the code for thermal design of civil building (MOHURD 2016), the requirements, such as for wall insulation, are less stringent in warmer climate zones. Thus, when the region is reassigned to a warmer climate zone, it will influence construction materials required, construction cost, energy demand, and energy efficiency of new buildings (Athalye *et al* 2016).

To examine the model-related uncertainties, the late-century changes of the building climate zones projected by the five individual models are compared in figure 5. The general spatial patterns of the projected changes are similar among the models, all featuring changes from zone 8 to zone 7 over the Tibetan Plateau, 3A to 2A south of the Yangtze River, and 7 to 6A, 6A to 5A, 4A to 3A, and 2A to 1A in eastern China. The spatial extent of areas influenced by such changes differ substantially among the models, and reaches 45%, 46%, 48%, 62% and 72% based on climate changes projected by the RegCM model driven by EC-EARTH, MPI-ESM-MR, NorESM1-M, CSIRO-Mk3-6-0 and HadGEM2-ES, respectively. The CSIRO-Mk3-6-0 and HadGEM2-ES models are the most sensitive due to the greater magnitude of warming in these two models (Wu and Gao 2020).

4. Conclusions and discussion

In this paper, using the definition described by the U.S. Department of Energy Pacific Northwest National Laboratory (PNNL), we investigate future changes in building climate zones based on five sets of high-resolution regional climate change projections under RCP4.5 scenario over East Asia. The main findings are summarized as follows:

(a) The building climate zones in China show a distinct latitudinal pattern over East China ranging from the very-hot climate zone in the south to the very cold climate zone in the north; subarctic climate zone is found in the western mountains including the Tibetan Plateau and cool dry climate zone is observed in the Tarim and Turpan basins. The five-model ensemble mean captures this spatial pattern well.
(b) Warming in the past several decades has already caused substantial northward shift of most climate zones in eastern China and a shrinking of the subarctic climate zones over the Tibetan Plateau. This has caused a change of building climate zone for over 18% of the country's land.
(c) Project future warming is expected to cause additional climate zone shifts similar to what has already been observed. The projected shift would influence 43% of the country's land by mid-century and 55% by late-century based on the five-model ensemble mean.

Large uncertainties in the spatial pattern of climate zones can originate from the GCMs boundary forcing, the RCP scenarios, and the RCMs. Multi-model ensemble of climate projections is an important and effective way to reduce these uncertainties (Giorgi *et al* 2009). While considering multiple GCMs, our study makes use of one RCM only. Adding other RCMs may reveal further uncertainties in projecting the future changes. While the bias correction method used in the study has some impact on the uncertainty, differences between the projected changes with and without bias correction indicate that uncertainties related to bias correction is rather low, influencing approximately 4% of the country land by the end of the century.

Compared with the previous climate classification methods that were developed for different application purpose, the climate zone classification used in this study is specifically designed for considerations related to building code and energy efficiency. The spatial distribution of building climate zones over China based on our results is similar to that based on the Köppen climate classification (Shi *et al* 2012) and the climate types developed by Zheng *et al* (2010), and thus can be used as an alternative to the existing methods. In this study the climate zone boundaries are entirely determined by climate factors; in practice, the climate zone boundaries should follow those of the municipal administration units to facilitate the implementation of building energy efficiency code by the local government.

Acknowledgments

Ying Shi was supported by the National Key Research and Development Program (2017YFA0605002), the

National Natural Science Foundation (41805063, 41991285 and 41375104) and the Climate Change Specific Fund of China (CCSF201925).

Data availability statement

The data that support the findings of this study are available upon reasonable request from the authors.

References

ANSI/ASHRAE Standard 169 2013 Climatic data for building design standards 104pp

Athalye R, Taylor T and Liu B, 2016. Impact of ASHRAE Standard 169-2013 on building energy codes and energy efficiency. ASHRAE and IBPSA-USA SimBuild 2016, Building Performance Modeling Conf. (Salt Lake City, UT, August 8–12)

Bai L J and Yang L 2018 Application of different zoning methods to climate zoning of building energy efficiency design *HV&AC* **48** 2–11 in Chinese

Bai L J, Yang L, Song B and Liu N 2020 A new approach to develop a climate classification for building energy efficiency addressing Chinese climate characteristics *Energy* **195** 116982

Baker B, Diaz H, Hargrove W and Hoffman F 2010 Use of the Köppen–Trewartha climate classification to evaluate climatic refugia in statistically derived ecoregions for the People's Republic of China *Clim. Change* **98** 113–31

Belda M, Holtanova E, Kalvova J and Halenka T 2016 Global warming-induced changes in climate zones based on CMIP5 projections *Clim. Res.* **71** 17–31

Bentsen M *et al* 2013 The Norwegian Earth System Model, NorESM1-M – part 1: description and basic evaluation of the physical climate *Geosci. Model Dev.* **6** 687–720

Cannon A J, Sobie S R and Murdock T Q 2015 Bias correction of GCM precipitation by quantile mapping: how well do methods preserve changes in quantiles and extremes? *J. Clim.* **28** 6938–59

Chen D L and Chen H W 2013 Using the Koppen classification to quantify climate variation and change: an example for 1901-2010 *Environ. Dev.* **6** 69–79

Collins W J *et al* 2011 Development and evaluation of an Earth-system model-HadGEM2 *Geosci. Model. Dev.* **4** 1051–75

de Castro M, Gallardo C, Jylha K and Tuomenvirta H 2007 The use of a climate-type classification for assessing climate change effects in Europe from an ensemble of regional climate models *Clim. Change* **81** 329–41

EBCAS (Editorial Board of Chinese Academy of Sciences) 1985 *Physical Geography in China: Climatology* (Beijing: Science Press) in Chinese

Emanuel K A 1991 A scheme for representing cumulus convection in large-scale models *J. Atmos. Sci.* **48** 2313–29

Eyring V, Bony S, Meehl G A, Senior C A, Stevens B, Stouffer R J and Taylor K E 2016 Overview of the Coupled Model Intercomparison Project Phase 6 (CMIP6) experimental design and organization *Geosci. Model. Dev.* **9** 1937–58

Feng S, Hu Q, Huang W, Ho C-H, Li R and Tang Z 2014 Projected climate regime shift under future global warming from multi-model, multi-scenario CMIP5 simulations *Glob. Planet. Change* **112** 41–52

Fernandez J P R, Franchito S H, Rao V B and Llopart M 2017 Changes in Koppen-Trewartha climate classification over South America from RegCM4 projections *Atmos. Sci. Lett.* **18** 427–34

Fu X Z, Zhang H L and Huang G D 2008 Discussion of climatic regions of building energy efficiency in China *HV&AC* **38** 44–47 in Chinese

Gao X J *et al* 2001 Climate change due to greenhouse effects in China as simulated by a regional climate model *Adv. Atmos. Sci.* **18** 1224–30

Gao X J *et al* 2018 Future changes of thermal comfort conditions over China *Atmos. Ocean. Sci. Lett.* **11** 291–9

Gao X J and Giorgi F 2008 Increased aridity in the Mediterranean region under greenhouse gas forcing estimated from high resolution simulations with a regional climate model *Glob. Planet. Change* **62** 195–209

Gao X J, Wang M L and Giorgi F 2013 Climate change over China in the 21st century as simulated by BCC_CSM1.1-RegCM4.0 *Atmos. Ocean. Sci. Lett.* **6** 381–6

Gao X J, Xu Y, Zhao Z C, Pal J S and Giorgi F 2006 On the role of resolution and topography in the simulation of East Asia precipitation *Theor. Appl. Clim.* **86** 173–85

Giorgi F *et al* 2012 RegCM4: model description and illustrative basic performance over selected CORDEX domains *Clim. Res.* **52** 7–29

Giorgi F, Jones C and Asrar G R 2009 Addressing climate information needs at the regional level: the CORDEX framework *WMO Bull.* **58** 175–83

Han Z Y, Shi Y, Wu J, Xu Y and Zhou B 2019 Combined dynamical and statistical downscaling for high-resolution projections of multiple climate variables in the Beijing-Tianjin-Hebei region of China *J. Appl. Meteorol. Clim.* **58** 2387–403

Han Z Y, Tong Y and Gao X J 2018 Correction based on quantile mapping for temperature simulated by the RegCM4 *Adv. Clim. Change Res.* **14** 331–40 in Chinese

Han Z Y, Zhou B T, Xu Y, Wu J and Shi Y 2017 Projected changes in haze pollution potential in China: an ensemble of regional climate model simulations *Atmos. Chem. Phys.* **17** 10109–23

Hazeleger W *et al* 2010 EC-Earth A seamless earth-system prediction approach in action *Bull. Am. Meteorol. Soc.* **91** 1357–63

He W P, Zhao S S, Wu Q, Jiang Y-D and Wan S 2019 Simulating evaluation and projection of the climate zones over China by CMIP5 models *Clim. Dyn.* **52** 2597–612

Holtslag A A, De Bruijn E I and Pan H L 1990 A high resolution air mass transformation model for short-range weather forecasting *Mon. Wea. Rev.* **118** 1561–75

IPCC 2013 Climate change 2013: the physical science basis *Contribution of Working Group I to the Fifth Assessment Report of the Intergovernmental Panel on Climate Change.* ed Field C B *et al*, ed T F Stocker, D H Qin, G K Plattner and M Tignor *et al* (Cambridge: Cambridge University Press) 1132

Iversen T *et al* 2013 The Norwegian earth system model, NorESM1-M-Part2: climate response and scenario projections *Geosci. Model Dev.* **6** 389–415

Jacob D *et al* 2012 Assessing the transferability of the regional climate model REMO to different coordinated regional climate downscaling experiment (CORDEX) regions *Atmos.* **3** 181–99

Jiang D B, Tian Z P and Lang X M 2016 Reliability of climate models for China through the IPCC Third to Fifth Assessment Reports *Int. J. Climatol.* **36** 1114–33

Jiang D B, Wang H J and Lang X M 2005 Evaluation of East Asian climatology as simulated by seven coupled models *Adv. Atmos. Sci.* **22** 479–95

Jungclaus J H, Fischer H, Haak H, Lohmann K, Marotzke J, Matei D, Mikolajewicz U, Notz D and von Storch J S 2013 Characteristics of the ocean simulations in the Max Planck Institute Ocean Model (MPIOM) the ocean component of the MPI-Earth system model *J. Adv. Model. Earth Syst.* **5** 422–46

Kiehl J T, Hack J J, Bonan G B, Boville B A, Williamson D L and Rasch P J 1998 The National Center for Atmospheric Research Community Climate Model: CCM3 *J. Clim.* **11** 1131–49

Kim M-K, Kim S, Kim J, Heo J, Park J-S, Kwon W-T and Suh M-S 2016 Statistical downscaling for daily precipitation in Korea using combined PRISM, RCM, and quantile mapping: part 1, methodology and evaluation in historical simulation *Asia-Pac. J. Atmos. Sci.* **52** 79–89

Köppen W *et al* 1936 Das geographische System der Klimate *Handbuch Der Klimatologie, Vol I, Part C*, ed Köppen W and Geiger H (Berlin: Gebrüder Borntraeger) pp 44

Kottek M, Grieser J, Beck C, Rudolf B and Rubel F 2006 World map of the Köppen-Geiger climate classification updated *Meteor. Z.* **15** 259–63

MCC (Ministry of Construction of China) 1993 *Standard of Climatic Regionalization for Architecture (GB 50178-93)* (Beijing: China Architecture & Building Press) 137pp in Chinese

MOHURD (Ministry of Housing and Urban-Rural Development of the People's Republic of China) 2016 *Code for Thermal Design of Civil Building (GB 50176-2016)* (Beijing: China Architecture & Building Press) 184pp in Chinese

Moss R H *et al* 2010 The next generation of scenarios for climate change research and assessment *Nature* **463** 747–56

Netzel P and Stepinski T 2016 On using a clustering approach for global climate classification *J. Clim.* **29** 3387–401

NMA (National Meteorological Administration) 1979 *Climatological Atlas for the People's Republic of China* (Beijing: Maps Press) in Chinese

NMA (National Meteorological Administration) 1994 *Climatological Resources Atlas for China* (Beijing: Sinomaps Press) in Chinese

NMA (National Meteorological Administration) 2002 *Climatological Atlas for the People's Republic of China* (Beijing: China Meteorological Press) in Chinese

Oleson K W *et al* 2008 Improvements to the Community Land Model and their impact on the hydrological cycle *J. Geophys. Res.* **113** G01021

Pal J S, Small E E and Eltahir E A 2000 Simulation of regional-scale water and energy budgets: representation of subgrid cloud and precipitation processes within RegCM *J. Geophys. Res.* **105** 29579–94

Pierce D W, Barnett T P, Santer B D and Gleckler P J 2009 Selecting global climate models for regional climate change studies *Proc. Natl Acad. Sci.* **106** 8441–6

Qian Y and Leung R L 2007 A long-term regional simulation and observations of the hydroclimate in China *J. Geophys. Res.* **112** D14104

Rahimi J, Khalili A and Butterbach-Bahl K 2019 Projected changes in modified Thornthwaite climate zones over Southwest Asia using a CMIP5 multi-model ensemble *Int. J. Climatol.* **39** 4575–94

Rotstayn L D*et al* 2010 Improved simulation of Australian climate and ENSO-related rainfall variability in a global climate model with an interactive aerosol treatment *Int. J. Climatol.* **30** 1067–88

Rubel F and Kottek M 2010 Observed and projected climate shifts 1901–2100 depicted by world maps of the Köppen-Geiger climate classification *Meteor. Z.* **19** 135–41

Shi Y, Gao X J and Wu J 2012 Projected changes in Koppen climate types in the 21st century over China *Atmos. Ocean. Sci. Lett.* **5** 495–8

Shi Y, Wang G L and Gao X J 2018 Role of resolution in regional climate change projections over China *Clim. Dyn.* **51** 2375–96

Stevens B *et al* 2012 Atmospheric component of the MPI-M earth system model: ECHAM6 *J. Adv. Model Earth Syst.* **5** 146–72

Taylor K E, Stouffer B J and Meehl G A 2012 An overview of CMIP5 and the experiment design *Bull. Am. Meteorol. Soc.* **93** 485–98

Tong Y *et al* 2017 Bias correction of daily precipitation simulated by RegCM4 model over China *Chin. J. Atmos. Sci.* **41** 1156–66 in Chinese

Tong Y, Gao X J, Han Z Y, Xu Y, Xu Y and Giorgi F 2020 Bias correction of temperature and precipitation over China for RCM simulations using the QM and QDM methods *Clim. Dyn.*

Trewartha G T and Horn L H 1980 *An Introduction to Climate* (New York: McGraw-Hill)

USDA Plant Hardiness Zone Map 2012. Agricultural Research Service, U.S. Department of Agriculture (https://planthardiness.ars.usda.gov/)

Wu J and Gao X J 2013 A gridded daily observation dataset over China region and comparison with the other datasets *Chin. J. Geophys.* **56** 1102–11 in Chinese

Wu J and Gao X J 2020 Present day bias and future change signal of temperature over China in a series of multi-GCM driven RCM simulations *Clim. Dyn.* **54** 1113–30

Xu Y, Gao X J and Giorgi F 2010 Upgrades to the reliability ensemble averaging method for producing probabilistic climate-change projections *Clim. Res.* **41** 61–81

Yu E T, Wang H J and Sun J Q 2011 A quick report on a dynamical downscaling simulation over China using the nested model *Atmos. Ocean. Sci. Lett.* **3** 325–9

Zhang X L and Yan X D 2014 Spatiotemporal change in geographical distribution of global climate types in the context of climate warming *Clim. Dyn.* **43** 595–605

Zhang X L, Yan X D and Chen Z J 2017 Geographic distribution of global climate zones under future scenarios *Int. J. Climatol.* **37** 4327–34

Zheng J Y, Yin Y H and Li B Y 2010 A new scheme for climate regionalization in China *Acta. Geogr. Sin.* **65** 3–12 in Chinese

Zhou B T, Wen Q H, Xu Y, Song L and Zhang X 2014 Projected changes in temperature and precipitation extremes in China by the CMIP5 multimodel ensembles *J. Clim.* **27** 6591–611

Zou L W and Zhou T J 2013 Near future (2016-40) summer precipitation changes over China as projected by a regional climate model (RCM) under the RCP8.5 emissions scenario: comparison between RCM downscaling and the driving GCM *Adv. Atmos. Sci.* **30** 806–18